GU J Sci, Part C, 10(4): 1026-1036 (2022)

Gazi University

Journal of Science

PART C: DESIGN AND TECHNOLOGY

http://dergipark.gov.tr/gujsc

The Attitude of ZnO/Al_2O_3 Film Produced by Ultrasonic Spray Pyrolysis under Thermal Annealing

Meryem POLAT GONULLU[1,*] Damla Dilara CAKIL Cemil CETINKAYA

[1]*Gazi University Faculty of Technology, Department of Metallurgical and Materials Engineering, 06500, Yenimahalle/ANKARA*

Article Info

Research article
Received: 30.06.2022
Revision: 10.09.2022
Accepted: 24.09.2022

Keywords

ZnO
Al2O3
Bilayer films
Spray Pyrolysis
Thermal annealing
Characterization

Abstract

Impact of annealing on structural, morphological, elemental, electrical, and optical properties of bilayer ZnO/Al_2O_3 films has been investigated. Bilayer films have been deposited on microscope slides by ultrasonic spray pyrolysis method at 350°C substrate temperature. Then, those films have been annealed at 400°C, 500°C, and 600°C under atmospheric conditions, respectively. Structural analysis has revealed that bilayer films have polycrystalline with hexagonal wurtzite structures of ZnO. Also, there is no other structures have been found like Zn-Al, etc. Morphological and elemental analyses have been presented that the alterations of surface, and diffusions of Al to ZnO layer. Cross-sectional images have revealed the film thicknesses are between 0.78-1.56 µm. Resistivity values of the films have been obtained between $6.78x10^1$ ohm-cm to 3.29 $x10^1$ ohm-cm. Optical method has been used for the calculation of optical band gap values of the films which are found between 3.17-3.25 eV. The results have revealed that annealing leads to diffusion from the bottom layer of Al_2O_3 of the material to the upper layer, ZnO. In addition, the properties of ZnO/Al_2O_3 films are still the focus of researchers.

1. INTRODUCTION

Bilayers or otherwise known as “laminates” at nano or micro scale films come out of alternating layers as metal oxides [1]. This layer-by-layer structured film design reveals unique properties according to single-layer film structures like electrical, optical, morphological, and photocatalytic properties. Each layer can have a specific thickness that arranges the film behavior. This bilayer film structure consists of different metal oxides like ZnO, ZnS, TiO_2, Al_2O_3, Fe_2O_3, CuO, etc, and can be used in many application areas like optoelectronic devices, solar cells, photocatalysis as a result of the unique properties of each structure [5-9]. In particular, bilayer films combined with these metal oxides are intended for use in optoelectronic applications. Among them, bilayer structures consisting of ZnO and Al_2O_3 layers have been attracting attention, recently [10-13]. Due to the optical properties like high transparency of ZnO and high specific surface area of Al_2O_3 layers, ZnO/Al_2O_3 bilayer/laminate films are especially useful for optical coatings [14, 15].

ZnO/Al_2O_3 bilayer films and derivatives can be produced by many techniques such as chemical vapor deposition (CVD), atomic layer deposition (ALD), sol-gel dip coating, and ultrasonic spray pyrolysis (USP) techniques [16-22]. However, production of bilayer ZnO/Al_2O_3 has been studied by few works and few production methods [23-26]. Ultrasonic spray pyrolysis is a low-cost, easy-used technique that enables to production of homogeneous films on different types of substrates in large areas. Also, this technique does not require vacuum, which is a great advantage. Adjustable production parameters like molarity of spraying solution chemicals, the flow rate of spraying, solutions, type of solvents such as alcohol and/or pure water, substrate temperature, and configurable spraying nozzle to substrate distance are other advantages of USP technique. However, the possibility of layered film production with USP and the fact that the studies in this

*Corresponding author, e-mail: meryempolat@gazi.edu.tr DOI:10.29109/gujsc.1137863

field are quite up-to-date and few contribute to the originality of the research to be conducted in the related field [27, 28].

In general, research is focused on the production and characterizations of optoelectronic, morphologic, and electrical properties of layered films by combining metal oxides. However, it is well known that annealing has great effects on layered film properties as in single-layered films. The crystallinity level, crystallite sizes, dislocations, and phase transformations may occur in the structure after the annealing process [2, 29]. According to production parameters like temperatures, chemicals, type of solvent, etc., it is well known that the crystallization of ZnO can occur at different phases with the effect of annealing while Al_2O_3 needs higher production temperatures [30-32].

Despite the importance of layer-by-layer films in optoelectronic applications, no study focusing on the investigation of some physical properties of "annealed double-layer films produced by ultrasonic spray pyrolysis" has been encountered so far. Hence, the present work focuses on investigating and determining the effect of annealing on structural, morphological, elemental, and optical alterations of bilayer ZnO/Al_2O_3 film produced by USP technique.

2.MATERIALS AND METHODS

Ultrasonic spray pyrolysis technique has been used for the production of ZnO/Al_2O_3 bilayer films on microscope slides. Glass substrates have been cleaned with detergent, ultra-pure water ($\rho \geq 15$ MΩcm), and ethanol before the film production, respectively. 0.1 M $Zn[(CH_3COO)_2Zn.2H_2O]$ (purity ≥99.999%, Sigma Aldrich) and $Al(NO_3)_3.9H_2O$ (purity ≥98%, Sigma Aldrich) have been used as a chemical source of spraying solution in ultra-pure water. These chemical solutions have been stirred for 30 minutes at room temperature and sprayed onto 350°C preheated microscope slide substrates, respectively. To create a bilayer structure, firstly, the aluminum solution has been sprayed onto microscope slides. Then, the zinc solution has been sprayed on the first/bottom layer that cooled down, in order to grow the ZnO layer. Flow rate of the solutions has been kept at 5 ml/min and controlled by a flowmeter during the spraying. Also, for 30 minutes using an ultrasonic nozzle total of 150 ml of starting solutions have been sprayed for each layer under the 1 bar air pressure as a carrier gas. After the bilayer film production, ZnO/Al_2O_3 film have been annealed at 400°C, 500°C, and 600°C, respectively in an atmosphere-controlled furnace.

The structural alterations of as-deposited and annealed ZnO/Al_2O_3 films have been studied by using Bruker D8 Advanced diffractometer (XRD) with CuK_α (1.5418 Å) radiation in the $20^o \leq 2\theta \leq 80^o$ range. The surface morphology, cross-sectional images with film thicknesses, and changes in the elemental distributions have been investigated by Jeol JSM 6060LV scanning electron microscope (SEM) and Energy Dispersive X-ray Spectrometer (EDX, IXRF system). Optical properties have been analyzed by Shimadzu UV-Visible model 2600 spectrophotometer in the range of 200 nm to 800 nm. Optical band gap values of all films have been obtained by an optical method. The resistivity measurements have been performed via van der Pauw method with square-shaped (1x1 mm^2) samples and ohmic contacts in the corner. Electrical contacts have been used for confirming the ohmic behavior by the current-voltage characteristics. The measurements have been made at room temperatures using Lakeshore Hall effect measurement system (HMS). The data have been analyzed using the QMSA technique. For simplicity, the films are coded as Z/A-As, Z/A-400, Z/A-500, and Z/A-600 according to the as-deposition and annealing temperature.

3.RESULTS AND DISCUSSION

XRD graphs of bilayer Z/A-As, and annealed Z/A-400, Z/A-500, and Z/A-600 films have been shown in Fig.1. XRD graphs present several diffractions at different intensities (remarked with a line equal to 1000 counts) that are well matched with the peaks related to the ZnO (ICDD: 36-1451). These several diffractions show the polycrystalline nature of the films. However, no diffraction belonging to the Al phases has been seen in the XRD pattern that is related to its crystallization behavior at high temperatures. Peaks specified diffracted from (100), (002), (101), (102), (110), (103), (200), (112), and (201) planes present the hexagonal wurtzite structure of ZnO. Research in the literature made by Tuzemen et.al. has presented almost a similar behavior for the crystallization of ZnO structure on Al_2O_3 coated glass substrates by RF magnetron sputter technique [14].

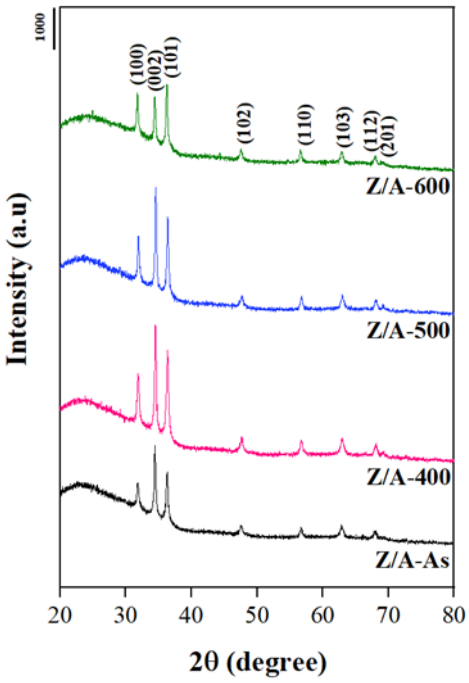

Figure 1. *XRD patterns of as-deposited and annealed bilayer ZnO/Al_2O_3 films*

From Table 1, it can be seen that the diffraction angles (2θ), intensities (I), interplanar spacing (d) with ICDD values, and β (full width half maximum) values of three intense diffraction peaks that present the alterations in the crystal structure according to annealing temperature. Among the three most intense peaks, the (002) diffraction plane has a higher crystallinity level after the as-deposited ZnO/Al_2O_3 film has been annealed at 400°C. However, all peaks exhibit the increasing peak intensity that indicates the improving crystal quality with the effect of annealing at 400°C. After the annealing temperature reaches 500°C, bilayer film presents almost the same crystalline behavior although the decreasing peak intensities. Nevertheless, when the annealing temperature reaches 600°C, the dominance of (101) diffraction plane increased and changes the crystal structure. In Table 2, the data such as texture coefficient (P), the crystallite size (D), and dislocation density (δ) values related to three major peaks have been given as a result of the mathematical calculations [33-35], and explanations on the subject are brought in below.

As seen in Table 2, calculations have revealed that Z/A-As, Z/A-400, and Z/A-500 films present the preferential orientation (P) remarked with bold type, through the (002) diffraction plane. When the bilayer Z/A-As film was annealed at 600°C, a sudden change occurred, and preferential orientation transform to the dominant growth directions through the (100) and (002) planes. These type changes indicate the co-growth of different phases in the crystal structure after the annealing process of bilayer film at 600°C. It can be seen from Table 2 that the crystallite sizes (D) have been changed between 31-39 nm that presenting the fluctuations in the crystallite sizes as a result of annealing. In another word, annealing at 400°C has caused a decrease to 34.83 nm in crystallite size while annealing at 500°C has caused an increase to 37.33 nm, and also at 600°C a decrease again to 31.52 nm. These fluctuations of crystallite sizes indicate the variable grain boundaries and so the number of defects in the film structure.

Table 1. *Structural parameters of as-deposited and annealed bilayer ZnO/Al_2O_3 films*

Sample	Miller Indice	2θ (º)	$2\theta_0$ (º)	I	I_0	d (Å)	d_0 (Å)	β (º)
	(100)	31.835	31.772	1755	58	2.8088	2.8143	0.289
Z/A-As	(002)	34.438	37.422	2631	45	2.6021	2.6033	0.209
	(101)	36.312	36.253	2006	101	2.4720	2.4759	0.305
	(100)	31.835	31.772	2384	58	2.8088	2.8143	0.284
Z/A-400	(002)	34.517	37.422	3539	45	2.5964	2.6033	0.239
	(101)	36.351	36.253	2936	101	2.4695	2.4759	0.307
	(100)	31.914	31.772	2181	58	2.8020	2.8143	0.268
Z/A-500	(002)	34.596	37.422	3307	45	2.5906	2.6033	0.223
	(101)	36.371	36.253	2627	101	2.4682	2.4759	0.264
	(100)	31.775	31.772	2141	58	2.8139	2.8143	0.178
	(002)	34.418	37.422	2059	45	2.6036	2.6033	0.264
Z/A-600	(101)	36.253	36.253	2334	101	2.4759	2.4759	0.240

Dislocation density values are seen in Table 2 and Fig 2 together with variations in crystallite sizes. From these values and images, it can be seen that the as-deposited film has minimum dislocation value according to annealed ones. Also, the highest annealing temperature has led to higher dislocation density values and so deteriorated crystal structure. It is estimated that the dislocation density increases due to the increase in the grain boundary per unit area while the crystal sizes decrease. This situation indicates transformations from compressive to tensile movements in the structure.

Table 2. *Calculated structural parameters of as-deposited and annealed bilayer ZnO/Al_2O_3 films*

Sample	P	D (nm)	δ (line/nm^2)	ρ (ohm-cm)
	0.82587	28.60	1.22E-03	
Z/A-As	**1.63204**	39.82	6.31E-04	6.78 E+01
	0.54209	27.43	1.33E-03	
	0.81877	29.11	1.18E-03	
Z/A-400	**1.60218**	34.83	8.24E-04	7.59 E+01
	0.57905	27.25	1.35E-03	
	0.81291	30.85	1.05E-03	
Z/A-500	**1.62479**	37.33	7.17E-04	5.3 E+01
	0.56229	31.69	9.96E-04	
	1.03673	46.43	4.64E-04	
Z/A-600	**1.31426**	31.52	1.01E-03	3.29 E+01
	0.64902	34.85	8.23E-04	

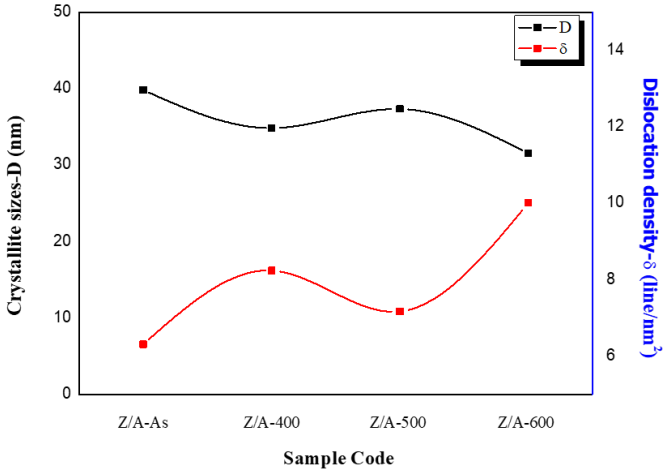

Figure 2. *Variations of crystallite sizes and dislocation density values belonging to the (002) diffraction plane*

Plan-view surface morphologies of Z/A-As, Z/A-400, Z/A-500, and Z/A-600 films have been investigated at X2500 and X5000 magnifications that are given in Fig 3 (a-h). Micrographs taken at X2500 magnification (Fig. 3 a-d) of all films exhibited agglomerations, cavitied areas, root-like formations, and cracks (indicated with red lines in Fig. 3 a), f), e), and d), respectively) especially film annealed at 600°C. Micrographs that have been taken at X5000 (Fig. 3 e-h) show the details of the film surface and these formations. For example, cavitied areas can be associated with droplet trails coming from spraying. However, root-like formations are associated with the temperature difference between the layers of film, evaporation of solvent during the production process, and losing the hydroxyl/alkoxy groups as a result of the heating process of this method in the literature and also been detailed in our earlier study [19, 36-39]. Cracks, as seen in the film annealed at 600°C, indicate structural deformations under the effect of higher annealing temperatures. To investigate these cracks, detailed images in different locations of the film have been taken. Results present the increasing crack formations (Fig. 3 d inset) in some regions accompanied by (Fig. 3 h inset) shrinkage. This situation may be correlated with the high thermal annealing temperatures and the loss of chemicals in the structure.

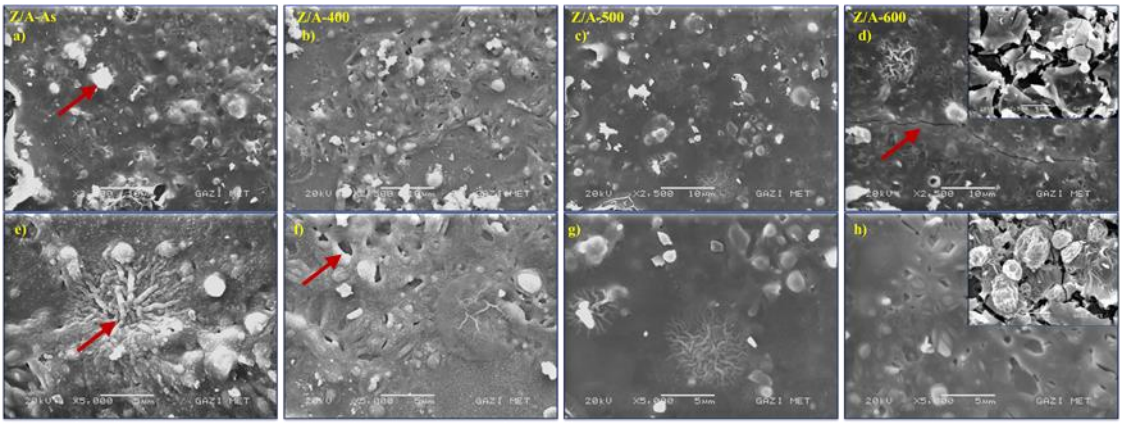

Figure 3. *Plan-view SEM images of as-deposited and annealed bilayer ZnO/Al_2O_3 films*

Cross-sectional SEM images of Z/A-As, Z/A-400, Z/A-500, and Z/A-600 films have been analyzed to determine the approximate film thicknesses and are given in Fig. 4 (a-d). From these figures, the average approximate thicknesses of all films have been determined as 1.25 µm; 776 nm; 1.49 µm; and 1.56 µm, respectively for Z/A-As, Z/A-400, Z/A-500, and Z/A-600 films. The decreasing thickness values for film annealed at 400°C may be associated with surface morphology, decreased roughness, and perhaps manufacturing conditions. Other studies on this subject have revealed the smooth, and homogeneous nanoscale film surface morphology, and thickness obtained from SEM and TEM images [14, 40-42].

However, it should be taken into account that the studies on ZnO/Al_2O_3 films have been exhibited by expensive vacuum production systems using gas-phase precursors, unlike spray pyrolysis.

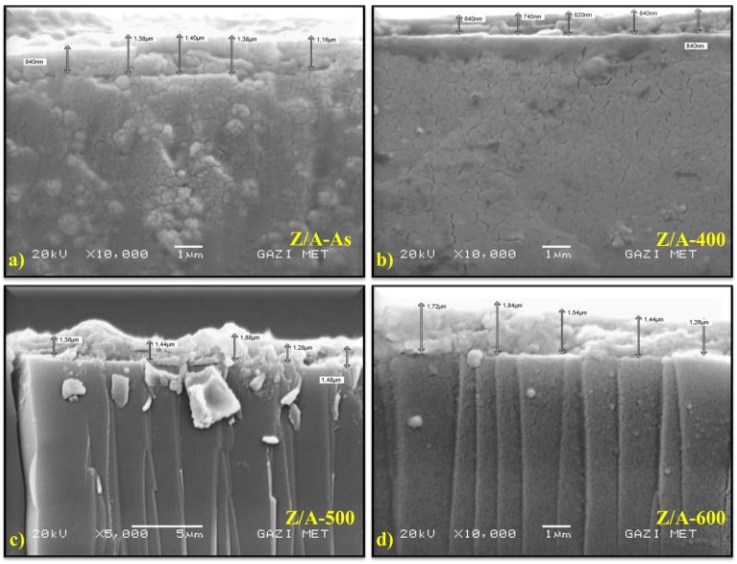

Figure 4. *Cross-sectional SEM images of as-deposited and annealed bilayer ZnO/Al_2O_3 films*

EDX analyses have been implemented on ZnO/Al_2O_3 films to understand the elemental behavior of layers after annealing. In figure 5, elemental investigations related to the Zn, Al, and O elements have been attempted to be determined from layers of ZnO/Al_2O_3 film numbered as 1, 2, and 3 points. It should be noted here that the layers have been selected and produced as Al_2O_3 on the bottom layer and ZnO on the upper layer during the spraying. Accordingly, 3 different points have been tried to be investigated for EDX analyses so as to be two layers and one junction region of films.

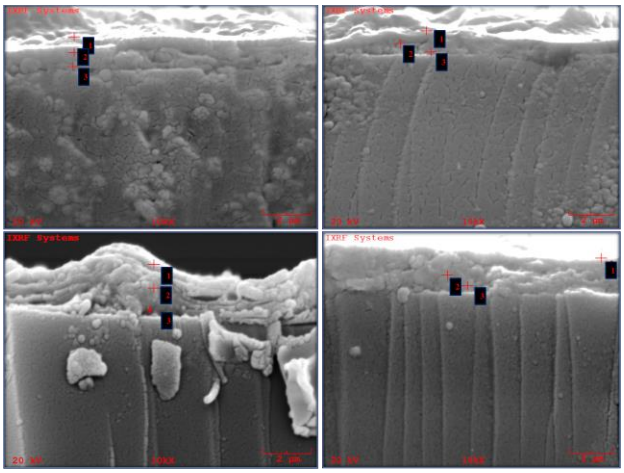

Figure 5. *EDX analysis regions of as-deposited and annealed bilayer ZnO/Al_2O_3 films*

Atomic weights (at %) of Zn, Al, and O elements from these points are listed in Table 3. From these selected points in the figures and analyzed results given in Table 3, it can be said that the 1st points present the decreasing zinc (Zn) concentrations under the effect of increasing annealing temperature. However, aluminum (Al) concentrations at these points are increasing with the increasing temperature. In the 2nd points, which we call the junction region, it can be seen that the Al concentrations are higher than in the first point which indicates the ZnO layer and increasing these values with annealing temperature as determined in the first points. Unlike the first points, a higher amount of Al concentration has been determined in these points, which can be attributed to the closeness of the junction region to the bottom aluminum layer. Considering the 3rd points, small concentrations of zinc have been determined. This can be attributed to the thickness/closeness of the layers and/or low precision of EDX measurement.

Consequently, it can be interpreted that all data indicates a higher amount of Al diffusions from the bottom layer to the top ZnO layer as a result of increasing annealing temperature.

***Table 3**. EDX measurement results of as-dep. and annealed bilayer ZnO/Al_2O_3 films.*

Materials	**As-dep.**			**400°C**			**500°C**			**600°C**		
Elements	**Zn**	**Al**	**O**	**Zn**	**Al**	**O**	**Zn**	**Al**	**O**	**Zn**	**Al**	**O**
1st Points	66.02	10.46	23.52	47.36	25.37	27.27	59.25	29.82	10.92	22.07	64.69	13.25
2nd Points	47.54	38.56	13.91	42.87	46.04	11.10	24.66	52.98	22.36	11.53	68.91	19.56
3rh Points	21.72	53.05	25.23	20.30	52.23	27.47	15.01	72.45	12.55	8.41	72.78	18.82

Electrical resistivity measurement results of ultrasonic spray pyrolyzed ZnO/Al_2O_3 films have been listed in Table 2. These results indicate that the annealing of ZnO/Al_2O_3 films has caused a decrease in the resistivity values of the films from 6.78×10^1 ohm-cm to 3.29×10^1 ohm-cm. In general, resistivity of the films is increased with decreasing crystallite sizes in the film due to the increasing grain boundary [43, 44]. In the current study, the resistivities of our films have almost the same values. Alterations in the coefficients could be associated with the structural changes as phase transformations from (002) to (101) diffraction planes, thicknesses of the films, surface morphology as porosity and/or roughness, defects in the film structure like Zn interstitials and O vacancies.

Figure 6 presents the absorption spectra (a) and optical band gap of as-deposited and annealed ZnO/Al_2O_3 films. Almost the same and constant absorbance values have been determined for all bilayer ZnO/Al_2O_3 films throughout the 400-800 nm wavelength as seen in Figure 6 a). When it comes to short wavelengths an abrupt increase in the absorbance values indicates the fundamental absorption edges have been obtained between the 375-400 nm wavelengths. These absorption edges also indicate the optical band gaps of these films. However, in all films, only the annealed at 600°C film has revealed a distinctive absorbance behavior that shifts to the higher wavelength which presents the red shift of the absorption edge. This shift of the absorption edge indicates the lower energy level for optical band gap values of the ZnO/Al_2O_3 films annealed at 600°C. Optical band gap values of the ZnO/Al_2O_3 films have been calculated by the optical method as a result of absorbance spectra. From Figure 6 b), it can be seen that the films have 3.25 eV, 3.19 eV, 3.21 eV, and 3.17 eV optical band gap energies for as-deposited, annealed at 400 °C, 500 °C, 600 °C, respectively. Determined optical band gap values present the decreasing energies for the films after the annealing according to as-deposited film and bulk ZnO which is important for optoelectronic applications. Also, obtained band gap results in the current study present decreasing values compared to the study performed by Tuzemen et. al. who found approximately 3.28eV band gaps for nano-thick films [14].

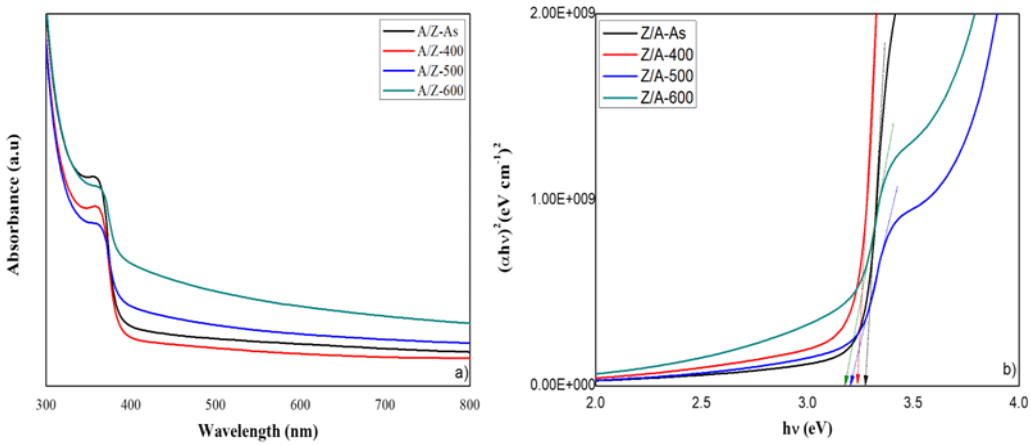

Figure 6. *Absorbance spectra and bandgap from the plot of $(\alpha h\nu)^2$ as a function of photon energy (hν) of as-deposited and annealed bilayer ZnO/Al_2O_3 films*

4.CONCLUSION

In this study, the attitude of ZnO/Al_2O_3 bilayer film produced by ultrasonic spray pyrolysis on microscope slides under thermal annealing has been investigated. Therefore, precursor solutions including aluminum and zinc have been sprayed on substrates, respectively. In this process, the second layer has been produced by waiting for it to cool after the first layer is produced. After the production, ZnO/Al_2O_3 film was subjected to thermal annealing under atmospheric conditions at 400 °C, 500 °C, 600 °C, respectively. XRD analyses have presented the improved crystallinity until the annealing temperature reaches 600 °C. After that, Z/A-600 film exhibited a decline in the crystal structure, with changing preferred orientation to dominant growth directions according to Z/A-As, Z/A-400, and Z/A-500 films. So, crystallite sizes and dislocation densities which are indicators of crystal quality and/or defects present the alterations at this annealing temperature as a result of phase transformation between (002) and (101) diffraction planes. Plan-view SEM images exhibit agglomerations, cavitied areas, root-like formations, and cracks on the surfaces especially film annealed at 600°C related to the higher temperature. EDX analyses revealed the elemental diffusion from the Al_2O_3 layer to the ZnO layer as the annealing temperature increased. Also, cross-sectional SEM images have shown the average thicknesses of all films between 776nm to 1.56 µm. Resistivity values of the films from 6.78×10^1 ohm-cm to 3.29×10^1 ohm-cm. Calculated optical band gap values of annealed bilayer films have shown that the decreasing values according to as-deposited ZnO/Al_2O_3 bilayer film is an expected situation for optoelectronic applications.

ACKNOWLEDGMENTS

No acknowledgment was declared by the author.

REFERENCES

[1] Rowlette, P. C., Wolden, C. A., Pulsed plasma-enhanced chemical vapor deposition of Al_2O_3–TiO_2 nanolaminates, Thin Solid Films, *518*(3337-3341), (2010).

[2] Khan, M. I., Imran, S., Saleem, M., Rehman, S. U., Annealing effect on the structural, morphological and electrical properties of TiO_2/ZnO bilayer thin films. Results in physics, 8(249-252), (2018).

[3] Besleaga, C., Stan, G. E., Galca, A. C., Ion, L., Antohe, S., Double layer structure of ZnO thin films deposited by RF-magnetron sputtering on glass substrate. Applied surface science, *258*(8819-8824) (2012).

[4] Yadav, H. M., and Kim, J. S., Fabrication of SiO_2/TiO_2 double layer thin films with self-cleaning and photocatalytic properties. Journal of Materials Science: Materials in Electronics, *27*(10082-10088) (2016).

[5] Lin, C. Y., Chen, J. G., Feng, W. Y., Lin, C. W., Huang, J. W., Tunney, J. J., Ho, K. C., Using a TiO_2/ZnO double-layer film for improving the sensing performance of ZnO based NO gas sensor. Sensors and Actuators B: Chemical, 157(361-367) (2011).

[6] Ding, K., Zhang, X., Ning, L., Shao, Z., Xiao, P., Ho-Baillie, A., ... and Jie, J., Hue tunable, high color saturation and high-efficiency graphene/silicon heterojunction solar cells with MgF2/ZnS double anti-reflection layer. Nano Energy, 46(257-265), (2018).

[7] Kanda, H., Uzum, A., Harano, N., Yoshinaga, S., Ishikawa, Y., Uraoka, Y., ... and Ito, S., Al_2O_3/TiO_2 double layer anti-reflection coating film for crystalline silicon solar cells formed by spray pyrolysis. Energy Science & Engineering, 4(269-276), (2016).

[8] Mahadik, M. A., Shinde, S. S., Mohite, V. S., Kumbhar, S. S., Moholkar, A. V., Rajpure, K. Y., ... and Bhosale, C. H., Visible light catalysis of rhodamine B using nanostructured Fe_2O_3, TiO_2 and TiO_2/Fe_2O_3 thin films. Journal of Photochemistry and Photobiology B: Biology, 133(90-98), (2014).

[9] Polyakov, B., Kuzmin, A., Vlassov, S., Butanovs, E., Zideluns, J., Butikova, J., ... and Zubkins, M., A comparative study of heterostructured $CuO/CuWO_4$ nanowires and thin films. Journal of Crystal Growth, 480 (78-84), (2017).

[10] Viter, R., Iatsunskyi, I., Fedorenko, V., Tumenas, S., Balevicius, Z., Ramanavicius, A., ... and Bechelany, M., Enhancement of electronic and optical properties of ZnO/Al_2O_3 nanolaminate coated electrospun nanofibers. The Journal of Physical Chemistry C, 120(5124-5132), (2016).

[11] Elam, J. W., Sechrist, Z. A., George, S. M., ZnO/Al_2O_3 nanolaminates fabricated by atomic layer deposition: growth and surface roughness measurements, Thin Solid Films, 414(43-55), (2002).

[12] Martínez-Castelo, J. R., López, J., Domínguez, D., Murillo, E., Machorro, R., Borbón-Nuñez, H. A., ... and Tiznado, H., Structural and electrical characterization of multilayer Al2O3/ZnO nanolaminates grown by atomic layer deposition. Materials Science in Semiconductor Processing, 71 (290-295), (2017).

[13] Ahn, C. H., Kim, S. H., Kim, Y. K., Lee, H. S., and Cho, H. K., Effect of post-annealing temperatures on thin-film transistors with ZnO/Al_2O_3 superlattice channels. Thin Solid Films, 584 (336-340) (2015).

[14] Tüzemen, E. Ş., Özer, A., Demir, İ., Altuntaş, İ., Şimşir, M., ZnO/Al_2O_3 layered structures deposited by RF magnetron sputtering on glass: growth characteristics, optical properties, and microstructural analysis. Journal of the Australian Ceramic Society, 57(1379-1388) (2021).

[15] Zahid, M. A., Khokhar, M. Q., Park, S., Hussain, S. Q., Kim, Y., and Yi, J., Influence of Al_2O_3/IZO double-layer antireflective coating on the front side of rear emitter silicon heterojunction solar cell. Vacuum, 200(110967), (2022).

[16] Purica, M., Budianu, E., Rusu, E., Danila, M. A., and Gavrila, R., Optical and structural investigation of ZnO thin films prepared by chemical vapor deposition (CVD). Thin Solid Films, 403(485-488), (2002).

[17] Di Mauro, A., Fragala, M. E., Privitera, V., and Impellizzeri, G., ZnO for application in photocatalysis: From thin films to nanostructures. Materials Science in Semiconductor Processing, 69(44-51), (2017).

[18] Kaneva, N. V., Dushkin, C. D., Preparation of nanocrystalline thin films of ZnO by sol-gel dip coating. Bulg Chem Commun, 43(259-263), (2011).

[19] Polat Gönüllü, M. The Effect of Annealing Technique on ZnO Film Properties. Gazi University Journal of Science, 35(618-629), (2022).

[20] Pradhan, S. K., Reucroft, P. J., Ko, Y., Crystallinity of Al_2O_3 films deposited by metalorganic chemical vapor deposition. Surface and Coatings Technology, 176(382-384), (2004).

[21] Nalcaci, B., Polat Gonullu, M., Insight of mechanical and morphological properties of ALD-Al_2O_3 films in point of structural properties. Applied Physics A, 127(1-10) (2021).

[22] Ateş, H., Polat Gonullu, M., Atomik Katman Biriktirme Tekniğine Genel Bakış: ZnO, TiO2 ve Al2O3 Filmlerin Üretimi. Gazi University Journal of Science Part C: Design and Technology, 7/3 (649-660) (2019).

[23] Khazamipour, N., Kabiri-Ameri-Aboutorabi, S., Asl-Solaimani, E., The structural, electrical and optical properties of ZnO/Al_2O_3 multilayer deposited on PET substrates by RF sputtering. Renewable energy, 49(275-277), (2013).

[24] Cui, G., Han, D., Dong, J., Cong, Y., Zhang, X., Li, H., ... and Wang, Y., Effects of channel structure consisting of ZnO/Al_2O_3 multilayers on thin-film transistors fabricated by atomic layer deposition. Japanese Journal of Applied Physics, 56(4S), (2017) 04CG03.

[25] Chaaya, A. A., Viter, R., Baleviciute, I., Bechelany, M., Ramanavicius, A., Gertnere, Z., ... and Miele, P., Tuning optical properties of Al_2O_3/ZnO nanolaminates synthesized by atomic layer deposition. The Journal of Physical Chemistry C, 118(3811-3819), (2014).

[26] Gonullu, M. P., Design and characterization of single bilayer ZnO/Al_2O_3 film by ultrasonically spray pyrolysis and its application in photocatalysis. Superlattices and Microstructures, 164(107113), (2022).

[27] Patil, P. S., Versatility of chemical spray pyrolysis technique. Materials Chemistry and physics, 59(185-198), (1999).

[28] Gonullu, M. P., Kose, S., On the Role of High Amounts of Mn Element in CdS Structure. Metallurgical and Materials Transactions A, 48(1321-1329), (2017).

[29] Khan, M. I., Ali, A., Effect of laser irradiation on the structural, morphological and electrical properties of polycrystalline TiO_2 thin films. Results in physics, 7(3455-3458), (2017).

[30] Garnier, J., Bouteville, A., Hamilton, J., Pemble, M. E., Povey, I. M., A comparison of different spray chemical vapour deposition methods for the production of undoped ZnO thin films. Thin Solid Films, 518(1129-1135), (2009).

[31] Bacaksiz, E., Parlak, M., Tomakin, M., Özçelik, A., Karakiz, M., Altunbaş, M., The effects of zinc nitrate, zinc acetate and zinc chloride precursors on investigation of structural and optical properties of ZnO thin films. Journal of Alloys and Compounds, 466(447-450), (2008).

[32] Jakschik, S., Schroeder, U., Hecht, T., Gutsche, M., Seidl, H., and Bartha, J. W., Crystallization behavior of thin ALD-Al_2O_3 films. Thin Solid Films, 425(216-220), (2003).

[33] Barrett, C. S., CS, B., and TB, M., Structure of metals, Crystallographic methods, principles and data, (1980).

[34] Callister, W. D., and Rethwisch, D. G., Materials science and engineering: an introduction (Vol. 9). (2018), New York: Wiley.

[35] Mamazza Jr, R., Morel, D. L., and Ferekides, C. S., Transparent conducting oxide thin films of Cd_2SnO_4 prepared by RF magnetron co-sputtering of the constituent binary oxides. Thin solid films, 484(26-33), (2005).

[36] Sutanto, H., Durri, S., Wibowo, S., Hadiyanto, H., Hidayanto, E., Rootlike morphology of ZnO:Al thin film deposited on amorphous glass substrate by sol-gel method. Physics Research International, 2016: 1-7, (2016).

[37] Navin, K. and Kurchania, R., Structural, Morphological and Optical Studies of Ripple Structured ZnO Thin Films. Applied Physics A: Materials Science and Processing, 121: 1155- 1161, (2015).

[38] Kwon, S. J. Park, J. H., Park, J. G., Wrinkling of sol–gel-derived thin Film. Physical Review E 71: 011604, (2005).

[39] Scherer, G. W., Sintering of sol–gel films. Journal of Sol-Gel Science and Technology 8(1): 353-363, (1997).

[40] Khazamipour, N., Kabiri-Ameri-Aboutorabi, S., Asl-Solaimani, E., The structural, electrical and optical properties of ZnO/Al2O3 multilayer deposited on PET substrates by RF sputtering. Renewable energy, 49, 275-27, (2013).

[41] Ahn, C. H., Kim, S. H., Kim, Y. K., Lee, H. S., Cho, H. K., Effect of post-annealing temperatures on thin-film transistors with ZnO/Al2O3 superlattice channels. Thin Solid Films, 584, 336-340, (2015).

[42] Choi, D. W., Kim, S. J., Lee, J. H., Chung, K. B., Park, J. S., A study of thin film encapsulation on polymer substrate using low temperature hybrid ZnO/Al2O3 layers atomic layer deposition. Current Applied Physics, 12, S19-S23, (2012).

[43] Huafu, Z., Hanfa, L., Aiping, Z., Changkun, Y., Influence of the distance between target and substrate on the properties of transparent conducting Al–Zr co-doped zinc oxide thin films. Journal of semiconductors, 30(11), 113002, (2009).

[44] Lu, J. G., Ye, Z. Z., Zeng, Y. J., Zhu, L. P., Wang, L., Yuan, J., Liang, Q. L., Structural, optical, and electrical properties of (Zn, Al) O films over a wide range of compositions. Journal of Applied Physics, 100(7), 073714, (2006).